Polydimethylsiloxane Microlens Arrays Fabricated Through Liquid-Phase Photopolymerization and Molding

Xuefeng Zeng and Hongrui Jiang, *Member, IEEE*

***Abstract*—We report on polydimethylsiloxane (PDMS) microlens arrays fabricated through liquid-phase photopolymerization and molding. The gist of this fabrication process is to form liquid menisci of variable radii of curvature at an array of apertures through pneumatic control, followed by photopolymerization under ultraviolet radiance. The resultant polymerized structures are then transferred to PDMS utilizing two molding steps. By adjusting the pneumatic pressure during the process, a single aperture array can be used to fabricate PDMS microlens arrays with variant focal lengths. The liquid menisci are formed by liquid–air interfaces that are pinned at the top edges of the apertures along hydrophobic–hydrophilic boundaries generated through surface chemical treatments. The microlens arrays are optically characterized. Variant focal lengths from 2.35 to 5.54 mm and f-numbers from 1.27 to 5.88, dependent on the diameter of apertures and the applied pressure to form the liquid menisci, are achieved with this relatively simple process and match well with the physical model. Owing to the formation from the liquid–air interfaces, the surface roughness of microlenses is measured to be around 25 nm. [2007-0293]**

***Index Terms*—Hydrophobic–hydrophilic boundary, microlens array, photopolymerization, pneumatic control, polydimethylsiloxane (PDMS).**

I. Introduction

MICROLENSES are important optical components and have been extensively studied for many years [1]–[6]. Among these microlenses, microlens arrays have found many applications, such as photolithography [7], [8], optical communications [9], [10], microimaging systems [2], [11], [12] and lab on chips [13]–[15]. Benefiting from the small surface roughness at immiscible interfaces involving liquids, the microlens surfaces formed in most fabrication processes are based on the liquid–liquid or liquid–air interfaces, including plastic hot intrusion [16], photoresist thermal reflow [2], [7], [14], [17]–[19], inkjet printing [20], and isotropic etching [14], [21]. However, these fabrication methods generally have limited flexibility in patterning microlenses with different focal lengths.

To combat this challenge, we present an approach to making polydimethylsiloxane (PDMS) microlens arrays through liquid-phase photopolymerization (LP^3) [22]–[24] and molding. LP^3 is used to generate polymer structures from liquid menisci at an aperture array as the mold of the microlens array, followed by two molding steps to transfer the convex lens shape to PDMS. The pneumatic pressure to form the liquid menisci can be adjusted for a specific focal length. Therefore, variant focal lengths and f-numbers of microlenses can be achieved using a single aperture array. The optical characterization of the resultant PDMS microlens arrays is also described.

II. Principle and Structures

Fig. 1 shows the basic configuration of the microlens array. The aperture array that is used to generate the microlens array is defined by a single photomask. The apertures are connected through a microchannel. One end of the microchannel is connected to a syringe pump and the other end to a pressure sensor, as shown in Fig. 1. Photopolymerizable and water-based liquid is flowed into the microchannel and pneumatically squeezed out from the apertures by operating the syringe pump to form liquid menisci at the liquid–air interfaces at the top edges of the apertures. The radii of curvature of these liquid menisci are determined by three factors: the difference between the applied pneumatic pressure and the atmospheric pressure, the surface tension, and the gravity of the liquid. Therefore, a specific radius of curvature, thus the focal length of the resultant microlenses, can be achieved by tuning the applied pneumatic pressure P_1 in the microchannel. The sidewalls and bottom surfaces of the apertures are chemically treated hydrophilic (the red lines in Fig. 1), while the top surfaces of the apertures are naturally hydrophobic, thereby pinning the liquid–air interfaces along the hydrophobic–hydrophilic boundaries at the top edges of the apertures. These liquid menisci are maintained in a certain convex shape through the pneumatic control and then photopolymerized under ultraviolet (UV) radiance to form the transferring molds. Due to its excellent light transparency and mechanical flexibility [15], [25], PDMS is used as the microlens material. In order to obtain convex PDMS microlens arrays, two molding steps are utilized to transfer the fabricated polymerized structures to PDMS.

Manuscript received December 7, 2007; revised April 4, 2008. First published August 1, 2008; current version published October 1, 2008. This work was supported in part by the U.S. National Science Foundation under Grant ECCS 0702095, by the U.S. Department of Homeland Security through a grant awarded to the National Center for Food Protection and Defense at the University of Minnesota under Grants N-00014-04-1-0659 and DHS-2007-ST-061-000003, and by Wisconsin Institutes for Discovery. Subject Editor H. Zappe.

The authors are with the Department of Electrical and Computer Engineering, University of Wisconsin—Madison, Madison, WI 53706 USA (e-mail: hongrui@engr.wisc.edu).

Color versions of one or more of the figures in this paper are available online at http://ieeexplore.ieee.org.

Digital Object Identifier 10.1109/JMEMS.2008.926139

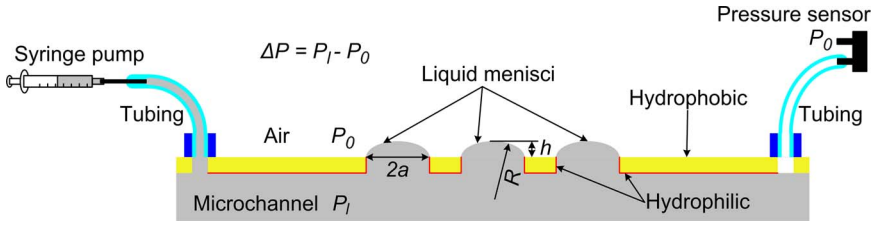

Fig. 1. Basic principle of forming a microlens array. The radii of curvature of liquid menisci, thus the focal lengths of the resultant microlenses, are adjusted by controlling the pneumatic pressure in the microchannel during the photopolymerization of the liquid menisci. The radius of the aperture is a; the height and the radius of curvature of the liquid menisci are h and R, respectively; and the pressures in the microchannel and in air are P_1 and P_0, respectively.

III. Fabrication of PDMS Microlens Arrays

The fabrication process of the microlens array is based on LP^3 and molding. In the whole process, four UV exposures for LP^3 and two molding steps are used. The first two masked UV exposures define the geometry of the aperture array and the microchannel, while the last two UV exposures are flood exposures that do not require photomasks. Two molding steps are utilized to transfer the polymerized structures to obtain the convex PDMS microlens arrays.

A. Equipment and Materials

Photopolymerization procedures are carried out using a desktop EXFO Acticure 4000 (EXFO Photonic Solutions, Inc., Missisauge, ON, Canada) UV light source. Photomasks used are printed high-resolution films (3000 dpi, Imagesetter, Inc., Madison, WI, USA).

Oxygen plasma treatments are carried out using a reactive ion etching (RIE) system (Unaxis 790, Unaxis Wafer Processing, Switzerland).

Pressures in the microchannel are manipulated by a syringe pump (Dual-syringe infusion/withdrawal pump, Cole Parmer Company, IL, USA) and are monitored by a pressure sensor (DC001NDC64, Honeywell Sensing and Control, Golden Valley, MN, USA). The output voltage from the pressure sensor is recorded by a digital multimeter (Test Bench 390A, B&K Precision Corporation, Yorba Linda, CA, USA).

There are two kinds of polymers used in this fabrication process: structural and removable. The detailed recipe can be found in previous publications [22], [23], [26], [27]. Structural polymers form microchannels and apertures, while removable polymers first form the liquid menisci, followed by photopolymerization, and are eventually dissolved. The structural photopolymerizable prepolymer mixture solution [isobornyl acrylate (IBA)] is similar to negative photoresists. Exposure to a UV light source without air causes IBA to cross link and the prepolymer mixture solution to solidify (called poly-IBA). The removable polymer, polyacrylamide (PAAm) hydrogel, formed or cured by cross-linking acrylamide using a cross-linker under UV radiance in air. Owing to abundant water in PAAm hydrogel prepolymer solution, it is water-based, and its surface tension is close to that of water.

Here, we use dithiothreitol (DTT, Sigma-Aldrich, St. Louis, MO, USA) to break the disulfide bonds in the cured PAAm hydrogel, slowly render it porous and ultimately dissolve it completely [26], [27]. First, 3-mL Tris buffer solution (molecular biology grade, Fisher Scientific, Inc., Pittsburgh, PA, USA) is added into 7-mL deionized (DI) water; then, 0.0154 g DTT is added into the solution. 1 M DTT solution is thus prepared [27]. PDMS prepolymer mixture is prepared by mixing the base with its curing agent (Dow Corning Corporation, Midland, MI, USA) at the weight ratio of 10 : 1. Before usage the PDMS prepolymer mixture is put in a vacuum chamber for 1 h to remove air bubbles.

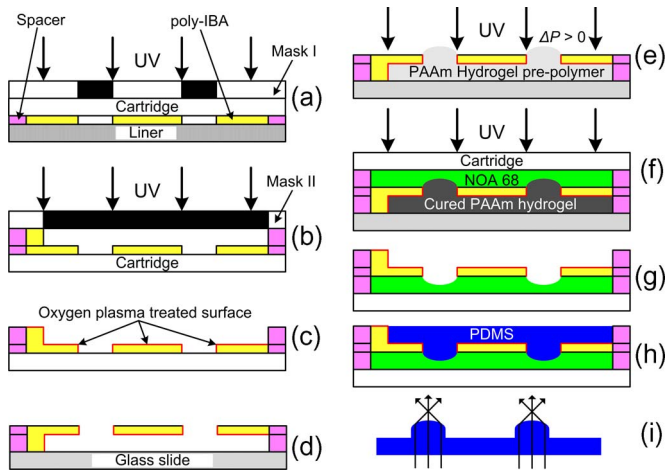

Fig. 2. Fabrication process of a microlens array. (a) IBA-based prepolymer mixture solution is flowed into a 250-μm-thick cartridge well, and the aperture array is photopatterned using LP^3; (b) a poly-IBA microchannel is photopatterned in a 350-μm-thick cavity using LP^3; (c) sidewalls and top surfaces of the poly-IBA plate are treated with oxygen plasma (red lines) to form the hydrophobic–hydrophilic pinning boundaries; (d) cartridge plate is peeled off and the poly-IBA plate is flipped over and bonded onto a glass slide; (e) liquid menisci of the water-based PAAm hydrogel prepolymer solution is formed under the pneumatic pressure and is polymerized under flood UV radiance; (f) nonshrinkable NOA 68 is applied onto the polymerized structures of PAAm hydrogel and precured under flood UV exposure; (g) cured PAAm hydrogel is dissolved in DTT solution, and the precured NOA 68 is next fully cured under UV radiance for 4 h to form a mold; (h) PDMS prepolymer mixture is applied onto the fully cured NOA 68 mold and cured for one day at room temperature; (i) PDMS microlens arrays are peeled off from the NOA 68 mold to complete the fabrication.

B. Fabrication Process Flow

Fig. 2 shows the fabrication process flow. First, an aperture array is made of poly-IBA in a polycarbonate cartridge well (40 $\times$ 22 mm, HybriWells, Grace Bio-Labs, Inc., Bend, OR, USA). The cartridge well consists of top cartridge plates and bottom liner plates adhered together by a 250-μm-thick spacer (double-sided adhesive tape) at the edge. IBA-based prepolymer mixture solution is flowed into the well using transfer

pipettes. The first film photomask (Mask I) is aligned on top of the cartridge plate and is exposed to UV light source (intensity, $I_{\mathrm{UV}} = 8.2$ mW/cm^2; time, $t = 23$ s) to form the poly-IBA aperture array [Fig. 2(a)]. The bottom liner plate is peeled off. Unpolymerized prepolymer solution is rinsed away with ethanol.

After the formation of the aperture array, the similar LP^3 procedure is used to form a poly-IBA microchannel on top of the aperture array. To define the height of the microchannel, 350-μm-thick spacers are used. Another film photomask (Mask II) is made contact to the top of the spacers as the top plate, and a cavity is formed. Under UV exposure ($I_{\mathrm{UV}} = 8.2$ mW/cm$^2, t = 26$ s), a microchannel forms on top of the aperture array [Fig. 2(b)]. Then, the photomask is peeled off, and ethanol is used to clean the structure.

Surfaces of poly-IBA are intrinsically hydrophobic (see Section V). An oxygen plasma treatment is carried out by RIE (power supply—50 W; oxygen flow rate—20.0 sccm; gas pressure—20 mtorr; treatment time—$t = 30$ s) to render surfaces of poly-IBA from hydrophobic to hydrophilic [28]. The top surfaces and the sidewalls of the apertures are treated [red lines in Fig. 2(c)], while the bottom surfaces keep naturally hydrophobic because of the protection from the cartridge plate [black lines in Fig. 2(c)]. Therefore, hydrophobic–hydrophilic boundaries are formed at the top edges of the apertures to later pin the liquid–air interfaces [Fig. 2(c)].

Next, the cartridge plate is peeled off, and the poly-IBA plate is bonded to a glass slide utilizing the treated hydrophilic side [Fig. 2(d)]. Epoxy (ITW Devcon, Danvers, MA, USA) is applied to the edge of the plate to avoid the leakage of the liquid.

Subsequently, one end of the microchannel is connected to a syringe pump and the other end to a pressure sensor by ethyl vinyl acetate microbore tubings (Cole Parmer Company, Vernon Hills, IL, USA), as shown in Fig. 1. The PAAm hydrogel prepolymer solution is flowed into the microchannel through the tubing and squeezed out from the apertures under the pneumatic pressure. Since the PAAm hydrogel prepolymer solution is water based, it is pinned at the hydrophobic–hydrophilic boundaries, and liquid menisci are formed at the liquid–air interfaces [Fig. 2(e)]. The radius of curvature of the resulting liquid menisci is controlled by the applied pressure in the microchannel. Simultaneously, the PAAm hydrogel prepolymer solution is flood exposed under UV radiance ($I_{\mathrm{UV}} = 25$ mW/cm$^2, t = 25$ s), and PAAm hydrogel is cured. During the exposure, the pressure in the microchannel is monitored by the pressure sensor and slightly adjusted to compensate for the shrinkage of PAAm hydrogel during its polymerization.

After being cured, PAAm hydrogel becomes white and opaque to the visible light. It also shrinks in air and changes shape. Therefore, the formed structures discussed above cannot be directly used as microlenses and need to be transferred to PDMS. Two molding steps are necessary for such a transfer to realize PDMS microlens arrays.

In order to reduce the shrinkage of polymerized PAAm hydrogel structures in air, nonshrinkable Norland Optical Adhesives (NOA) 68 (Norland Products, Inc., Cranbury, NJ, USA) is poured on top of the cured PAAm hydrogel immediately after its polymerization. A cartridge plate is put on top of NOA 68 and is supported by 1-mm-thick spacers [Fig. 2(f)]. NOA 68 is then precured under flood UV exposures ($I_{\mathrm{UV}} = 25$ mW/cm$^2, t = 10$ min).

Afterward, the entire polymer structures on glass slides are cut off, and the cured PAAm hydrogel is dissolved in 1 M DTT solution for 2 h, while precured NOA 68 maintains the shape of the polymerized structures [Fig. 2(g)]. The dissolved hydrogel is removed with ethanol and DI water. In order to avert the influence of uncured molecules in this precured NOA 68 during PDMS curing, the entire structures are next cured again under UV radiance ($I_{\mathrm{UV}} = 25$ mW/cm^2) for 4 h to form a fully cured NOA 68 mold for the microlens array. PDMS prepolymer mixture is next poured onto the mold and cured for one day at room temperature. After PDMS is fully cross-linked, it is peeled off from the NOA 68 mold, and a microlens array is completed [Fig. 2(i)].

IV. Physical Model of Microlenses

In order to obtain the relationship between the focal length of the fabricated microlenses and the applied pneumatic pressure, a physical model based on the equilibrium between the gravity G, the surface tension force F_{s}, and the applied pressure difference ΔP, between the pressure in the microchannel P_1, and atmospheric pressure P_0, is presented. The effect of the diameter of apertures on the radius of curvature of the liquid menisci is also studied. In this model, we assume that the radius of the apertures is a; the diameter of the apertures is d (equal to $2a$); the height and the radius of curvature of the liquid menisci are h and R, respectively (Fig. 1).

The focal length f of the microlenses is decided by the radius of curvature of the liquid menisci R and the refractive index of the lens material n given in

$$f = \frac{R}{n-1}. \tag{1}$$

Here, PDMS is the lens material; its refractive index is 1.416 at the wavelength of 610 nm [29].

When the PAAm hydrogel prepolymer solution is squeezed out from the apertures to form the liquid menisci, the gravity of each meniscus is

$$G = \frac{\pi}{3}\rho g\left(R - \sqrt{R^2 - a^2}\right)\left(R^2 + a^2 - R\sqrt{R^2 - a^2}\right) \tag{2}$$

where ρ is the mass density of the PAAm hydrogel prepolymer solution, and g is the acceleration of gravity equal to 9.8 m/s^2.

The surface tension force F_{s} between the PAAm hydrogel prepolymer solution and air is

$$F_{\mathrm{s}} = 2\frac{\gamma}{R}a^2 \tag{3}$$

where γ is the surface tension of the PAAm hydrogel prepolymer solution.

The force due to the pressure difference between this hydrogel prepolymer solution and air F is given as

$$F = \pi a^2 \cdot \Delta P \tag{4}$$

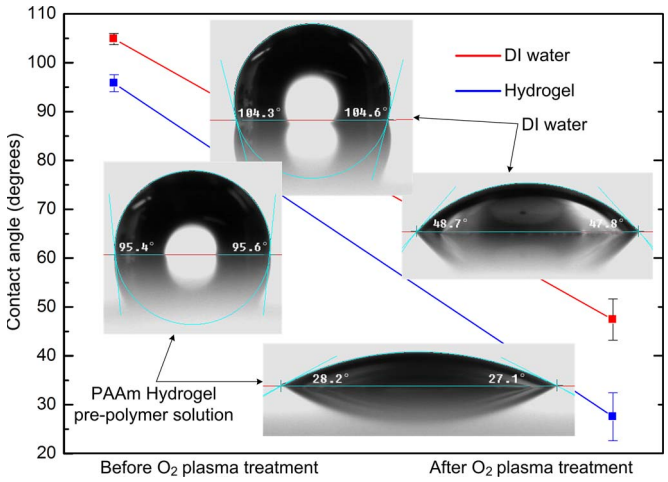

Fig. 3. Contact angles of DI water and PAAm hydrogel prepolymer solution on the same poly-IBA surface before and after oxygen plasma treatment. The contact angles of DI water and PAAm hydrogel prepolymer solution change from $104.9^\circ \pm 1.2^\circ$ to $47.4^\circ \pm 4.2^\circ$, and from $95.8^\circ \pm 1.8^\circ$ to $27.5^\circ \pm 4.9^\circ$, respectively. Error bars, $\pm$ s.d.

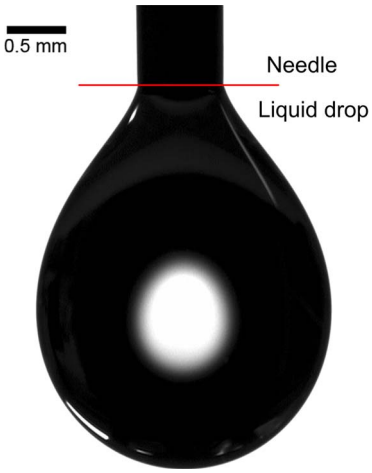

Fig. 4. Side-view image of a drop of PAAm hydrogel prepolymer solution at the end of a dosing needle, taken with a CCD camera installed on the goniometer. The surface tension of the PAAm hydrogel prepolymer solution is measured and calculated to be 58.6 ± 0.35 dyn/cm.

where

$$\Delta P = P_1 - P_0. \tag{5}$$

Therefore, the total forces onto a liquid meniscus of the PAAm hydrogel prepolymer are balanced among F, F_s, and G given in

$$F - F_s = G. \tag{6}$$

Substitute (2)–(4) into (6) and we have

$$\Delta P = \frac{1}{3a^2}\rho g\left(R - \sqrt{R^2 - a^2}\right) \times \left(R^2 + a^2 - R\sqrt{R^2 - a^2}\right) + 2\frac{\gamma}{R}. \tag{7}$$

The relationship between R and ΔP can be solved from (7) numerically. When R is substituted into (1), the focal length

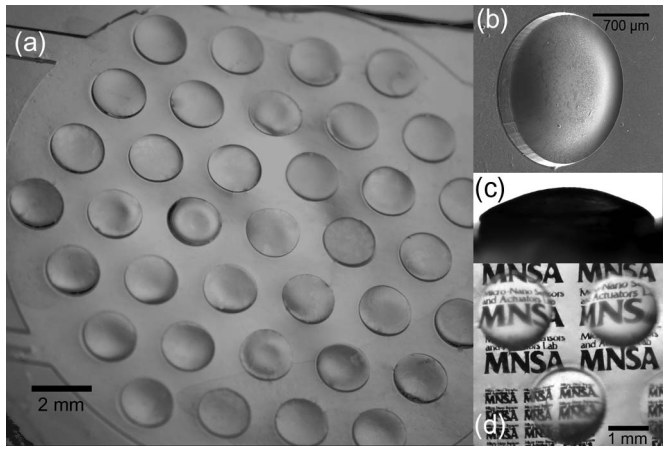

Fig. 5. (a) Optical image of a microlens array, taken with a stereomicroscope from an oblique angle. (b) SEM image of one microlens taken from a 40° angle. (c) Side-view image of the same microlens taken with a goniometer. (d) Magnified image of an object (the laboratory logo "MNSA") using the microlens array. The diameter of each microlens is 1.8 mm.

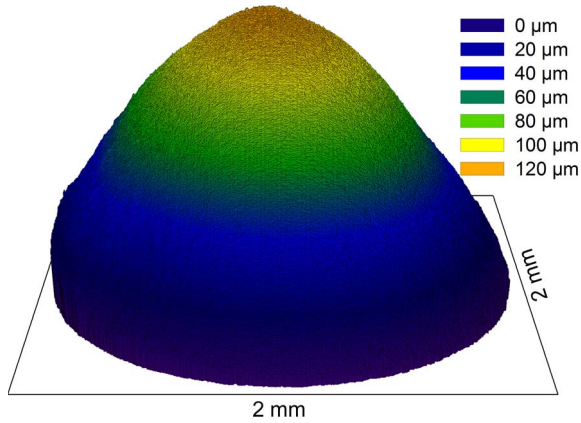

Fig. 6. Three-dimensional optical profile of a microlens taken by a white-light interferometer. The diameter of the microlens is 1.8 mm. The area scanned by the interferometer is 2×2 mm. The image is nonisometric and is elongated in the z-axis to clearly show the surface topography.

of the microlens arrays can be obtained as a function of the diameter of the microlenses and the applied pressure difference, which will be shown in Fig. 8 in Section V.

Note that if the gravity is neglected, hence $G = 0$ in (6), R and its corresponding f become independent of a and are given as

$$R = \frac{2\gamma}{\pi \cdot \Delta P} \tag{8a}$$

$$f = \frac{2\gamma}{(n-1)\,\pi \cdot \Delta P}. \tag{8b}$$

V. Experiments and Results

A. Contact Angles Measurements

Surfaces of poly-IBA are intrinsically hydrophobic and can be rendered hydrophilic after the oxygen plasma treatment. The surface energy of a solid surface can be defined by a contact

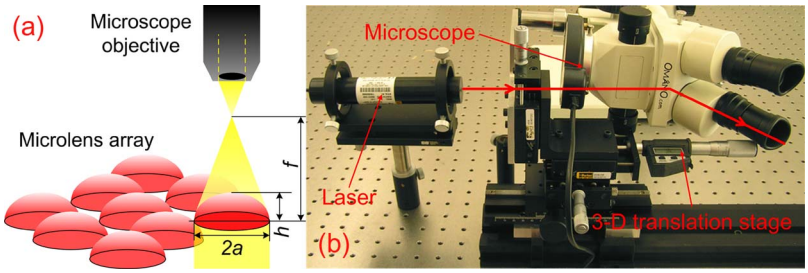

Fig. 7. (a) Schematic and (b) photo of the focal length measurement setup used. A collimated laser light at the wavelength of 633 nm illuminates from the bottom of the microlens arrays. A microscope is first focused on the base surface surrounding the microlenses as the zero point. Next, the focal point of a microlens is determined by finding the minimum image of the incident laser beam spot when moving the stage along the optical axis. The distance moved is the focal length of the microlens.

angle between a liquid and the solid surface [30], [31]. In order to compare the wettability of poly-IBA surfaces before and after the oxygen plasma treatment, contact angles of two different liquids, DI water and the PAAm hydrogel prepolymer solution, on these two surfaces are measured by a goniometer (OCA 15+, DataPhysics Instruments, Inc., Germany). Fig. 3 shows the change in the contact angles of DI water and the PAAm hydrogel prepolymer solution on the same poly-IBA surface before and after the oxygen plasma treatment. The error bars indicate the standard deviation of contact angles in each test. For DI water, the contact angle changes from $104.9^\circ \pm 1.2^\circ$ to $47.4^\circ \pm 4.2^\circ$, while for the PAAm hydrogel prepolymer solution, it changes from $95.8^\circ \pm 1.8^\circ$ to $27.5^\circ \pm 4.9^\circ$.

B. Surface Tension of the PAAM Hydrogel Prepolymer Solution

The surface tension of the PAAm hydrogel prepolymer solution is measured by a goniometer using a pendant drop method [31]. A drop of the PAAm hydrogel prepolymer solution is formed at the lower end of a dosing needle. The shape of the drop results from two forces: the gravity elongates the drop, and the surface tension holds the drop in spherical form to minimize the surface area. The equilibrium between these two forces is mathematically described by the Young–Laplace equation. To mathematically analyze the shape of the drop, the gravity must be calculated. Therefore, it is necessary to know the mass density difference between the drop phase and the surrounding medium.

The mass density of the PAAm prepolymer hydrogel solution is obtained by measuring the weight and the volume and found to be 0.987 g/mL. Fig. 4 shows a side-view image of a drop of the PAAm hydrogel prepolymer solution at the end of a needle (25 μL, Hamilton Company, Reno, NV, USA), taken with a charge-coupled device (CCD) camera installed on the goniometer. Surface profiles of the drop are extracted from the image, and the surface tension is calculated using the Young–Laplace equation. For the PAAm hydrogel prepolymer solution, the surface tension is 58.6 ± 0.35 dyn/cm.

C. Images of Microlenses

Fig. 5 shows the optical image of a typical microlens array, the scanning electron microscope (SEM) image, the side-view image of one microlens, and the magnified image of an object

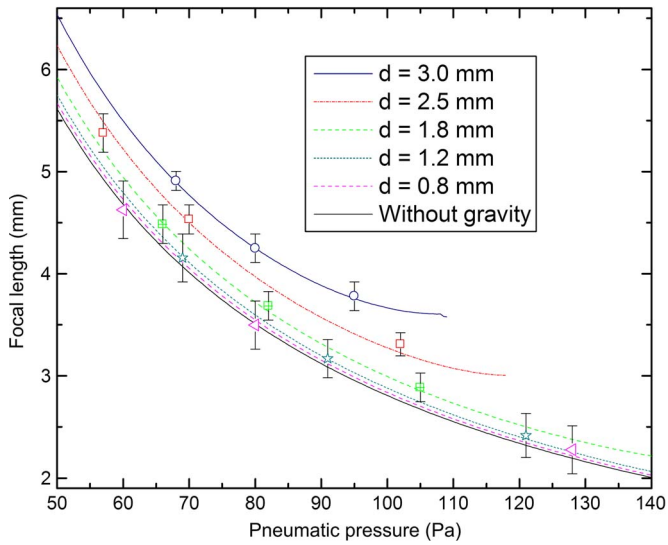

Fig. 8. Focal length f of the microlens arrays as a function of the pneumatic pressure ΔP and the diameter of apertures d. The curves are calculated from (7) and (8b). The measured focal length varies from 5.54 ($\Delta P = 57$ Pa and $d = 2.5$ mm) to 2.35 mm ($\Delta P = 121$ Pa and $d = 1.2$ mm). Error bars, $\pm$ s.d.

(laboratory logo) using the microlens array. The diameter of each microlens in the array is 1.8 mm. The optical image is taken with a stereomicroscope (Nikon SMZ1500, Nikon Instruments, Inc., Melville, NY, USA) from an oblique angle. The SEM image is taken with JEOL JSM-6100 (Tokyo, Japan) from a 40° angle. The side-view image is taken with the goniometer. The magnified image of the object "MNSA" is taken with the stereoscope from the top. The logo is printed on a transparent film. The film is under the microlens array, and the distance between them is 3 mm.

D. Three-Dimensional Profile and Surface Roughness of Microlenses

The profile of one microlens and the root-mean-square (rms) value on the surface of a microlens array are obtained by a white-light interferometer (Zygo NewView 6300, Zygo Corporation, Middlefield, CT, USA). Fig. 6 shows a 3-D optical interferometric profile of a typical microlens. The area scanned by the interferometer is 2×2mm. The image is nonisometric and elongated in the z-axis to clearly show the surface topography. The microlens is precoated with a thin layer of aluminum to obtain a clear interferometric image. RMS values

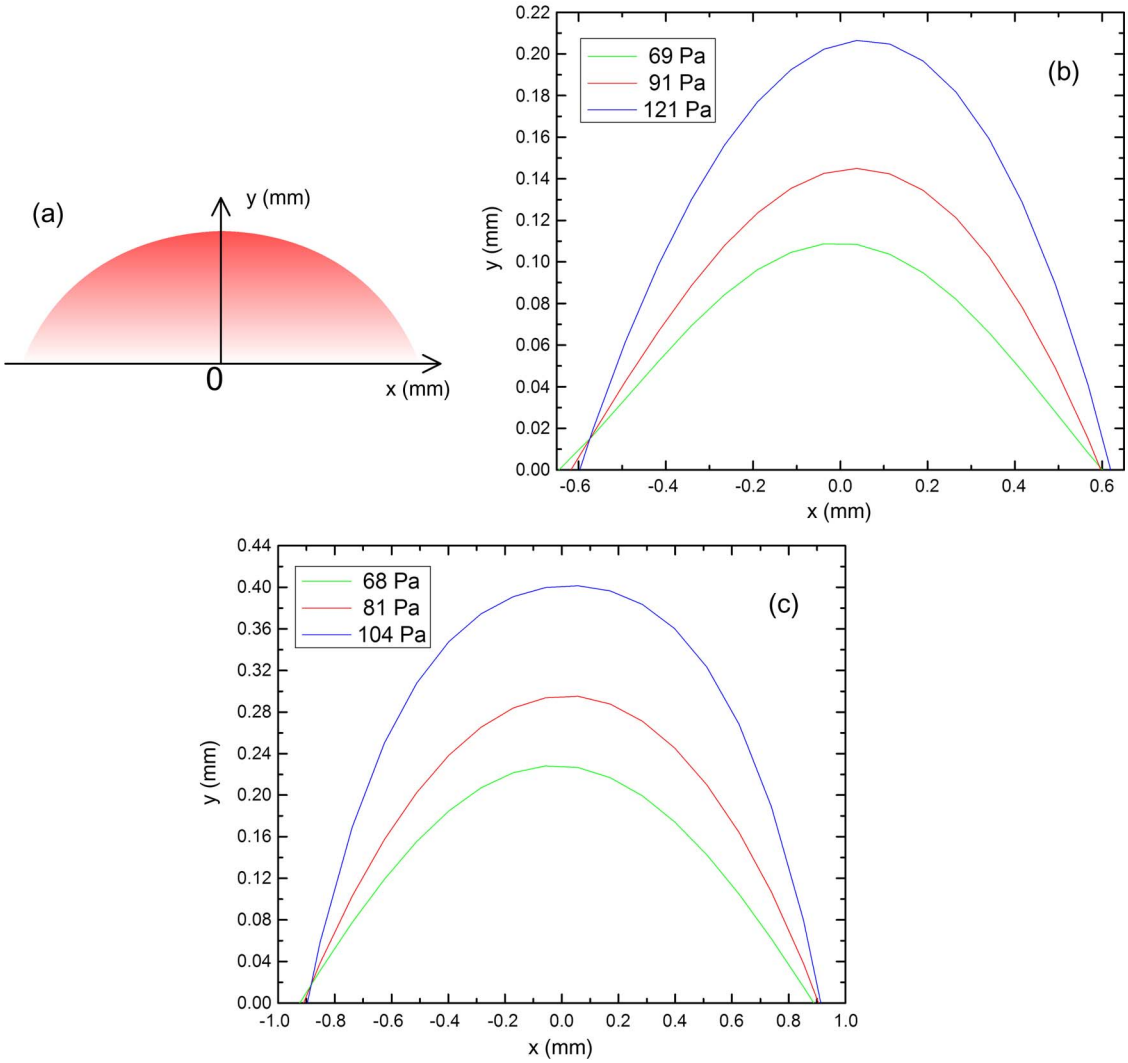

Fig. 9. (a) Cross-sectional schematic and (b and c) plots of surface profiles of the microlenses. The surface profiles of the microlenses are extracted from their 3-D interferometric profiles with two typical diameters of apertures. (b) 1.2 mm. (c) 1.8 mm. The plots are nonisometric and are elongated in the z-axis.

on spherical surfaces at the top of the microlenses and those on the base surfaces surrounding the microlenses are also measured by the interferometer. The typical values are 25 nm and 107 nm, respectively. Because spherical surfaces at the top of microlenses are formed from the liquid–air interfaces, the surface roughness is similar to that reported using other fabrication methods [5], [18] and is better than 1/10 wavelength from UV to infrared. Since transferred from the surfaces of cartridge plates, the base surfaces surrounding the microlenses are rougher than the spherical surfaces at the top of microlenses.

E. Focal Length Measurements

A focal length measurement setup is schematically shown in Fig. 7(a). The measurement setup is mounted on an optical table, and a picture is shown in Fig. 7(b). A collimated light at a wavelength of 633 nm from a laser (JDS Uniphase 1107, JDS Uniphase Corporation, Santa Rosa, CA, USA) illuminates from the bottom of the microlens array. Microlens arrays are mounted on and are moved by a 3-D translation stage (Parker Hannifin Corporation, Cleveland, OH, USA). First, a microscope (The Microscope Store, LLC, Wirtz, VA, USA) is focused on the base surfaces surrounding the microlenses as the zero point. Next, the stage is moved along the optical axis, and the focal point is decided by finding the minimum image in the microscope. Thus, this moving distance from the zero point to the focal point is the focal length of the microlenses.

The focal lengths of the fabricated microlens arrays with varying diameters of the apertures d and applied pneumatic pressure difference ΔP are measured and are plotted in Fig. 8. Error bars indicating the standard deviations in the focal lengths of the arrays are also shown. By solving (1) and (7), f as a function of ΔP, and d is plotted in a set of curves, also shown in Fig. 8. In our experiments, d varies from 0.8 to 3.0 mm, and ΔP varies from 57 to 121 Pa. As a result, f varies from 5.54 mm ($\Delta P = 57$ Pa and $d = 2.5$ mm) to 2.35 mm ($\Delta P = 121$ Pa and $d = 1.2$ mm) depending on d and ΔP. The calculated focal length matches well with the experimental data throughout the whole range shown in Fig. 8.

The curve without the gravity in Fig. 8 is calculated from (8b). As d increases, the effect of the gravity increases [see (7)], and the curve deviates more from that without the gravity.

TABLE I
SPHERICAL ABERRATION AND CORRESPONDING POLYNOMIAL COEFFICIENTS OF MICROLENSES WITH DIFFERENT DIAMETERS OF APERTURES AND PRESSURES

Diameter of aperture		1.2 mm			1.8 mm		
Pressures (Pa)		121	91	69	104	81	68
Polynomial coefficient	x	0.05584	0.32470	-0.00349	0.01657	0.01157	-0.01427
	x^2	-0.50623	-0.43234	-0.38709	-0.25537	-0.33424	-0.31628
	x^3	0.11387	-0.10644	-0.01177	-0.00550	-0.01594	0.007070
	x^4	-0.11504	0.10669	-0.26959	-0.02780	-0.02718	0.04700
Spherical aberration (μm)		2.021	1.722	1.354	0.331	0.612	0.671

The f-number $f/\#$ or the inverse of the relative aperture, can be calculated using f and d:

$$f/\# = \frac{f}{d}. \tag{9}$$

Based in Fig. 8, $f/\#$ is calculated and is between 1.27 ($\Delta P = 95$ Pa and $d = 3.0$ mm) and 5.88 ($\Delta P = 60$ Pa and $d = 0.8$ mm).

F. Spherical Aberration

Fig. 9(a) shows the cross-sectional schematic of a microlens, and Fig. 9(b) and (c) shows the surface profiles of six typical fabricated microlenses with different focal lengths from as many lens arrays (one lens from each array). The center of the microlens is set as the zero point, as shown in Fig. 9(a). These plots of the surface profiles are extracted from the 3-D interferometric profiles obtained for the microlenses (refer to Fig. 6). The diameters of apertures are 1.2 [Fig. 9(b)] and 1.8 mm [Fig. 9(c)], respectively. The curves of the surface profiles are fitted using fourth-order polynomials [15]. The polynomial coefficients are listed in Table I. The spherical aberrations of the microlenses are obtained from an optical simulation tool (Zemax SE, ZEMAX Development Corporation, Bellevue, WA, USA) utilizing the fitted polynomial coefficients of the curves and are also listed in Table I. From the data, the spherical aberration of the microlenses fabricated in our presented methods is on the order of 1 μm.

VI. CONCLUSION

We have demonstrated a relative simple method to fabricate PDMS microlens arrays using LP^3 and molding. Liquid menisci of PAAm hydrogel prepolymer solution at liquid–air interfaces are first formed, followed by photopolymerization under UV radiance to obtain the mold for the microlenses. The polymerized molding structures made of PAAm hydrogel are then transferred to PDMS to form the microlens arrays. The liquid–air interfaces are pinned at hydrophobic–hydrophilic boundaries at the top edges of the apertures. The radii of curvature of these menisci can be adjusted to a specific value by pneumatic pressure control. Hence, a single aperture array can be used to fabricate multiple microlens arrays with different focal lengths. The fabricated PDMS microlens arrays are optically characterized. Their focal lengths range from 2.35 to 5.54 mm and f-numbers from 1.27 to 5.88. The experimental data match well with the physical model. Due to the attribute of the liquid–air interfaces, the surface roughness of the microlenses is around 25 nm and is better than 1/10 wavelength of most light spectrum.

In future studies, we plan to fabricate microlens arrays with larger number and smaller size of microlenses to improve the fill factor. We will also investigate on methods to improve the pressure uniformity in the channel and the shrinkage of hydrogel to enhance the uniformity in the shape of the lenses and to improve the shape of the molds to reduce spherical aberrations. In addition, we will integrate such microlens arrays with other optical components, such as shutters, optical fibers, and waveguides. This fabrication method based on LP^3 and molding could potentially be extended to manufacture complex curved microstructures [32].

ACKNOWLEDGMENT

The authors would like to thank the following people at the University of Wisconsin—Madison: R. K. Noll at the Materials Science Center for his assistance in taking SEM images, Prof. D. Beebe and his group for offering access to their facilities, and Dr. L. Dong and Dr. S. Sridharamurthy for their insightful discussions. H. Jiang would like to thank the 3M Corporation for his Non-Tenured Faculty Award.

REFERENCES

[1] D. Daly, *Microlens Arrays*. Boca Raton, FL: CRC Press, 2000.
[2] K. H. Jeong, J. Kim, and L. P. Lee, "Biologically inspired artificial compound eyes," *Science*, vol. 312, no. 5773, pp. 557–561, Apr. 2006.
[3] L. Dong, A. K. Agarwal, D. J. Beebe, and H. Jiang, "Adaptive liquid microlenses activated by stimuli-responsive hydrogels," *Nature*, vol. 442, no. 7102, pp. 551–554, Aug. 2006.
[4] Y. Lu, Y. D. Yin, and Y. N. Xia, "A self-assembly approach to the fabrication of patterned, two-dimensional arrays of microlenses of organic polymers," *Adv. Mater.*, vol. 13, no. 1, pp. 34–37, Jan. 2001.
[5] J. Chen, W. S. Wang, J. Fang, and K. Varahramyan, "Variable-focusing microlens with microfluidic chip," *J. Micromech. Microeng.*, vol. 14, no. 5, pp. 675–680, May 2004.
[6] H. J. Shin, M. C. Pierce, D. Lee, H. Ra, O. Solgaard, and R. Richards-Kortum, "Fiber-optic confocal microscope using a MEMS scanner and miniature objective lens," *Opt. Express*, vol. 15, no. 15, pp. 9113–9122, Jul. 2007.
[7] M. H. Wu and G. M. Whitesides, "Fabrication of diffractive and micro-optical elements using microlens projection lithography," *Adv. Mater.*, vol. 14, no. 20, pp. 1502–1506, Oct. 2002.

[8] C. Y. Chang, S. Y. Yang, M. S. Wu, L. T. Jiang, and L. A. Wang, "A novel method for fabrication of plastic microlens array with aperture stops for projection photolithography," *Jpn. J. Appl. Phys. 1, Regul. Rap. Short Notes*, vol. 46, no. 5A, pp. 2932–2935, May 2007.
[9] H. Hamam, "A two-way optical interconnection network using a single mode fiber array," *Opt. Commun.*, vol. 150, no. 1–6, pp. 270–276, May 1998.
[10] S. Eitel, S. J. Fancey, H. P. Gauggel, K. H. Gulden, W. Bachtold, and M. R. Taghizadeh, "Highly uniform vertical-cavity surface-emitting lasers integrated with microlens arrays," *IEEE Photon. Technol. Lett.*, vol. 12, no. 5, pp. 459–461, May 2000.
[11] S. Kuiper and B. H. W. Hendriks, "Variable-focus liquid lens for miniature cameras," *Appl. Phys. Lett.*, vol. 85, no. 7, pp. 1128–1130, Aug. 2004.
[12] S. H. Chen, X. J. Yi, L. B. Kong, M. He, and H. C. Wang, "Monolithic integration technique for microlens arrays with infrared focal plane arrays," *Infrared Phys. Technol.*, vol. 43, no. 2, pp. 109–112, Apr. 2002.
[13] L. Dong and H. Jiang, "Tunable and movable liquid microlens *in situ* fabricated within microfluidic channels," *Appl. Phys. Lett.* vol. 91, no. 4, art. no. 041 109, Jul. 2007.
[14] J. C. Roulet, R. Volkel, H. P. Herzig, E. Verpoorte, N. F. de Rooij, and R. Dandliker, "Fabrication of multilayer systems combining microfluidic and microoptical elements for fluorescence detection," *J. Microelectromech. Syst.*, vol. 10, no. 4, pp. 482–491, Dec. 2001.
[15] N. Chronis, G. L. Liu, K. H. Jeong, and L. P. Lee, "Tunable liquid-filled microlens array integrated with microfluidic network," *Opt. Express*, vol. 11, no. 19, pp. 2370–2378, Sep. 2003.
[16] L.-W. Pan, X. Shen, and L. Lin, "Microplastic lens array fabricated by a hot intrusion process," *J. Microelectromech. Syst.*, vol. 13, no. 6, pp. 1063–1071, Dec. 2004.
[17] M. H. Wu and G. M. Whitesides, "Fabrication of two-dimensional arrays of microlenses and their applications in photolithography," *J. Micromech. Microeng.*, vol. 12, no. 6, pp. 747–758, Nov. 2002.
[18] W. Moench and H. Zappe, "Fabrication and testing of micro-lens arrays by all-liquid techniques," *J. Opt. A, Pure Appl. Opt.*, vol. 6, no. 4, pp. 330–337, Apr. 2004.
[19] A. Jain and H. K. Xie, "An electrothermal microlens scanner with low-voltage large-vertical-displacement actuation," *IEEE Photon. Technol. Lett.*, vol. 17, no. 9, pp. 1971–1973, Sep. 2005.
[20] H. Choo and R. S. Muller, "Addressable microlens array to improve dynamic range of Shack-Hartmann sensors," *J. Microelectromech. Syst.*, vol. 15, no. 6, pp. 1555–1567, Dec. 2006.
[21] K. Wang, K.-S. Wei, M. Sinclair, and K. F. Böhringer, "Micro-optical components for a MEMS integrated display," in *Proc. 12th IWPSD*, Chennai, India, 2003.
[22] A. K. Agarwal, S. S. Sridharamurthy, D. J. Beebe, and H. Jiang, "Programmable autonomous micromixers and micropumps," *J. Microelectromech. Syst.*, vol. 14, no. 6, pp. 1409–1421, Dec. 2005.
[23] A. K. Agarwal, D. J. Beebe, and H. Jiang, "Integration of polymer and metal microstructures using liquid-phase photopolymerization," *J. Micromech. Microeng.*, vol. 16, no. 2, pp. 332–340, Feb. 2006.
[24] D. J. Beebe, J. S. Moore, Q. Yu, R. H. Liu, M. L. Kraft, B. H. Jo, and C. Devadoss, "Microfluidic tectonics: A comprehensive construction platform for microfluidic systems," *Proc. Nat. Acad. Sci. U.S.A.*, vol. 97, no. 25, pp. 13 488–13 493, Dec. 2000.
[25] Y. N. Xia and G. M. Whitesides, "Soft lithography," *Annu. Rev. Mater. Sci.*, vol. 28, pp. 153–184, 1998.
[26] S. S. Sridharamurthy, A. K. Agarwal, D. J. Beebe, and H. Jiang, "Dissolvable membranes as sensing elements for microfluidics based biological/chemical sensors," *Lab Chip*, vol. 6, no. 7, pp. 840–842, May 2006.
[27] S. S. Sridharamurthy, L. Dong, and H. Jiang, "A microfluidic chemical/biological sensing system based on membrane dissolution and optical absorption," *Meas. Sci. Technol.*, vol. 18, no. 1, pp. 201–207, Jan. 2007.
[28] L. Dong, A. K. Agarwal, D. J. Beebe, and H. Jiang, "Variable-focus liquid microlenses and microlens arrays actuated by thermoresponsive hydrogels," *Adv. Mater.*, vol. 19, no. 3, pp. 401–405, Feb. 2007.
[29] D. A. Chang-Yen, R. K. Eich, and B. K. Gale, "A monolithic PDMS waveguide system fabricated using soft-lithography techniques," *J. Lightw. Technol.*, vol. 23, no. 6, pp. 2088–2093, Jun. 2005.
[30] R. R. A. Syms, E. M. Yeatman, V. M. Bright, and G. M. Whitesides, "Surface tension-powered self-assembly of microstructures—The state-of-the-art," *J. Microelectromech. Syst.*, vol. 12, no. 4, pp. 387–417, Aug. 2003.
[31] *Description of the Analytical Method for Characterizing the Surface Energy and Polarity of Liquid and Solid Contact Adhesives*, Dataphysics Inc., Filderstadt, Germany. [Online]. Available: http://www.dataphysics.de/pdf/App8e.pdf
[32] J. A. Bauer, T. A. Saif, and D. J. Beebe, "Surface tension driven formation of microstructures," *J. Microelectromech. Syst.*, vol. 13, no. 4, pp. 553–558, Aug. 2004.

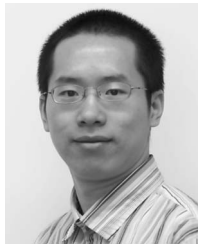

Xuefeng Zeng received the B.S. degree in microelectronic technology from Tianjin University, Tianjin, China, in 2002, the M.S. degree in electronic science and technology from Tsinghua University, Beijing, China, in 2005, and the M.S. degree in electrical and computer engineering in 2007 from the University of Wisconsin, Madison, where he is currently working toward the Ph.D. degree in electrical and computer engineering.

His research interests include the optical microlenses with the fixed or adaptive focal length, microfluidics, and responsive hydrogels.

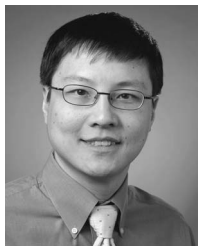

Hongrui Jiang (S'98–M'02) received the B.S. degree in physics from Peking University, Beijing, China, and the M.S. and Ph.D. degrees in electrical engineering from Cornell University, Ithaca, NY, in 1999 and 2001, respectively.

He is currently an Assistant Professor with the Department of Electrical and Computer Engineering, a Faculty Affiliate with the Department of Biomedical Engineering, and a Faculty Member of the Materials Science Program, University of Wisconsin (UW), Madison. Before he joined the faculty at UW, he was a Postdoctoral Researcher with the Berkeley Sensor and Actuator Center, University of California—Berkeley, Berkeley, from 2001 to 2002. His research interests are in microfabrication technology, biological and chemical microsensors, microactuators, optical MEMS, smart materials and micro/nanostructures, lab on a chip, and biomimetics and bioinspiration.

Dr. Jiang received the National Science Foundation CAREER Award and the Defense Advanced Research Projects Agency Young Faculty Award in 2008.